GEOPHYSICAL RESEARCH LETTERS, VOL. 30, NO. 4, 1157, doi:10.1029/2002GL016191, 2003

Nonlinear evolution of dust waves driven by cross-field electron currents

Wayne A. Scales and Gyoo Soo Chae

Bradley Department of Electrical and Computer Engineering, Virginia Tech, Blacksburg, Virginia, USA

Received 29 August 2002; revised 16 December 2002; accepted 17 January 2003; published 19 February 2003.

[1] The nonlinear evolution of dust waves generated by a low-frequency Hall current instability in a magnetized collisional dusty plasma is investigated with theory and nonlinear numerical simulations. This instability is believed to have broad applications to irregularity production in regions where dust is present in the earth's ionosphere such as noctilucent clouds and meteor trails. The instability is driven by an electron $\vec{E} \times \vec{B}$ current and is an analog, in the dust acoustic type wave regime, of the well-known Farley-Buneman instability. The results indicate that the instability nonlinearly saturates with dust heating and the production of secondary waves that propagate in a direction perpendicular to the primary dust acoustic type waves. *INDEX TERMS:* 2439 Ionosphere: Ionospheric irregularities; 2471 Ionosphere: Plasma waves and instabilities; 6944 Radio Science: Nonlinear phenomena; 7839 Space Plasma Physics: Nonlinear phenomena.

Citation: Scales, W. A., and G. S. Chae, Nonlinear evolution of dust waves driven by cross-field electron currents, *Geophys. Res. Lett., 30*(4), 1157, doi:10.1029/2002GL016191, 2003.

1. Introduction

[2] The investigation of the role cross-field electron current two-stream instabilities have in producing irregularities in the earth's ionosphere has had a long and rich history. In particular, the Farley-Buneman instability has been studied extensively over the past four decades due to its role in producing irregularities in the earth's E-region [*Kelley*, 1989]. Recently, significant progress in understanding its nonlinear evolution has lead to the interpretation of many unresolved issues associated with its application [*Oppenheim et al.*, 1996; *Otani and Oppenheim*, 1998].

[3] The increasing awareness of the existence of charged dust in the earth's mesosphere implies that a wide variety of new possibilities for irregularity generation mechanisms remain to be investigated. For instance, mechanisms for the production ofirregularities associated with noctilucent clouds [*Havnes et al.*, 1996; *Cho and Rottger*, 1997] and meteor trails [*Kelley et al.*, 1998], which both consist of charged dust, most likely involve dust waves. A low-frequency Hall current instability LFHI that involves the production of dust acoustic type waves by electron $\vec{E} \times \vec{B}$ currents has been recently investigated [*Rosenberg and Shukla*, 2000, 2002]. An important advantage of this plasma irregularity generation mechanism is that the critical electron drift may be significantly less than the ion sound speed and therefore much less than the critical drift of the standard Farley-Buneman instability. The LFHI shows much promise for interpreting fundamental irregularity generation mechanisms associated with regions of charged dust in the ionosphere as well as basic processes in dusty plasmas. However, just as an understanding of the nonlinear evolution of the Farley-Buneman instability has been crucial for its application in interpreting irregularity production, the same is expected of the LFHI. For instance, in applying the LFHI to interpreting experimentally observed irregularity spatial scales [*Rosenberg and Shukla*, 2000], an understanding of the nonlinear saturated state of the waves is expected to be as significant as the predictions of linear theory alone. The object of the present work is to investigate the nonlinear evolution of the LFHI by using nonlinear numerical simulation models. Emphasis will be placed on investigating saturation mechanisms and parameters that characterize the waves in a nonlinear saturated steady state.

0094-8276/03/2002GL016191

2. Plasma Model and Linear Theory

[4] A model consisting of a three species plasma with electrons, ions, and charged dust grains in a two-dimensional plane perpendicular to the background magnetic field $\vec{B}$ is considered. An external electric field $\vec{E}_0$ is applied to the plasma and produces an $\vec{E}_0 \times \vec{B}$ drift v_E on the electrons. The continuity equation for the fluid electrons is given by $\partial n_e/\partial t + \nabla \cdot (n_e \vec{v}_e) = 0$. The electron inertia is neglected, therefore, the electron momentum equation reduces to

$$0 = q_e\left(\vec{E}_0 + \vec{E} + \vec{v}_e \times \vec{B}\right) - \frac{\nabla p_e}{n_e} - \nu_{en} m_e \vec{v}_e \qquad (1)$$

where q_e and m_e are the electron charge and mass and ν_{en} is the electron-neutral collision frequency. Also, $p_e = n_e k_B T_e$ is the electron pressure where T_e is the electron temperature and k_B is Boltzman's constant. The wave electric field $\vec{E}$ is derivable from the electrostatic potential ϕ; $E = -\nabla\phi$.

[5] The unmagnetized fluid ions have continuity equation $\partial n_i/\partial t + \nabla \cdot (n_i \vec{v}_i) = 0$. The momentum equation is $\partial \vec{v}_i/\partial t + (\vec{v}_i \cdot \nabla)\vec{v}_i = q_i \vec{E}/m_i - \nabla p_i/m_i n_i - \nu_{in} m_i v_i$, where q_i and m_i are the ion charge and mass. Also $p_i = n_i k_B T_i$ is the ion pressure where T_i is the ion temperature. The ion-neutral collision frequency is ν_{in}.

[6] The unmagnetized dust particles are treated with the Particle-In-Cell PIC method. The dust is assumed to be collisional with dust-neutral collision frequency ν_{dn}. The dust collisions are implemented by using a Langevin approach [*Winske and Rosenberg*, 1998]. Poisson's equation, $\epsilon_0 \nabla^2 \phi = -(q_e n_e + q_i n_i + Q_d n_d)$ where $Q_d n_d$ denotes the dust charge density and ϵ_0 denotes the vacuum permitivity, is used to calculate ϕ. The numerical techniques are

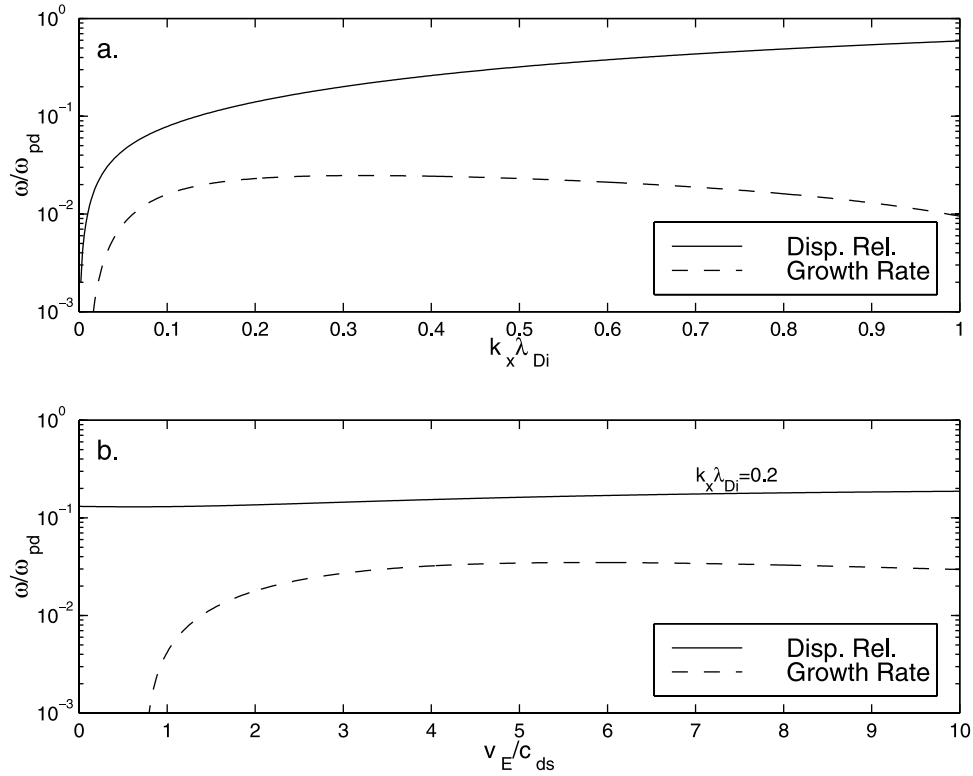

Figure 1. Linear growth rate calculations of the LFHI with parameters stated in the text.

described in previous work [*Chae et al.*, 2000; *Scales et al.*, 2001].

[7] The dispersion relation for the numerical model just described can be calculated from the usual expression $1 + \chi_e + \chi_i + \chi_d = 0$ where $\chi_{e,i,d}$ are the electron, ion, and dust susceptibilities, respectively. The susceptibilities may be written as $\chi_e = i\omega_{pe}^2\nu_{en}/\Omega_{ce}^2(\omega - kv_E + i\nu_{en}k^2\rho_e^2)$, $\chi_i = 1/k^2\lambda_{Di}^2$ and

$$\chi_d = \frac{1}{k^2\lambda_{Dd}^2}\{1 + \xi_d Z(\xi_d)\}\left\{1 + \frac{i\nu_{dn}}{\sqrt{2}kv_{td}}Z(\xi_d)\right\}^{-1} \qquad (2)$$

where ω_{pe} (Ω_{ce}) is the electron plasma (cyclotron) frequency, ρ_e is the electron cyclotron radius, λ_{Di} (λ_{Dd}) is the ion (dust) Debye length, $\xi_d = (\omega + i\nu_{dn})/\sqrt{2}kv_{td}$, v_{td} is the dust thermal velocity, and Z is the Fried and Conte plasma dispersion function.

[8] Figure 1a shows the variation of the frequency ω_r and growth rate γ with $k\lambda_{Di}$ while Figure 1b shows the variation with v_E. The frequency in Figure 1a can be seen to follow an approximate analytical expression for dust acoustic type waves $\omega_r \approx kc_{ds}/\sqrt{1 + k^2\lambda_{Di}^2}$ where $c_{ds} = \lambda_{di}\omega_{pd}$ is the dust acoustic speed and ω_{pd} is the dust plasma frequency. The critical drift for marginal stability in Figure 1b can be approximated to be $v_E^{crit} \approx c_{ds}/\sqrt{1 + k^2\lambda_{Di}^2 + T_i n_e/T_e n_i}$. The parameters used are chosen to fall within the regime considered in past work on the LFHI [*Rosenberg and Shukla*, 2000, 2002] which has been proposed to have important applications to noctilucent clouds and meteor trails. It should be noted that a reduced dust-ion mass ratio $m_d/m_i = 1000$ (rather than a realistic value of $\sim 10^7$) is used to make the model computationally feasable but will not make qualitative changes in the nonlinear evolution. Here $T_e = T_i = T_d$ and $n_i/n_e = 0.5$. The plasma is charge neutral $n_e + n_i + Z_d n_d = 0$ where Z_d is the number of charges on the dust grain. The dust is taken to be positively charged and $Z_d = +40$. The value $v_E = 2.5c_{ds}$ is used for the calculation in Figure 1a. The value of $k\lambda_{Di} = 0.20$, (which corresponds to mode 4 in the simulations), is considered in Figure 1b. For simplicity $\nu_{dn} = 0$ here. The qualitative nonlinear evolution of the LFHI is not altered, however, the effects on the wave saturation levels will be discussed shortly. It can be shown that the final parameter needed to determine the strength of the instability is $\alpha = \omega_{pe}^2\nu_{en}/\Omega_{ce}^2\omega_{pd}$ which is taken to be $\alpha = 20.0$. In the previous calculations, α is considerably larger primarily due to the realistic value of m_d/m_i used. The primary effect is an increase in the value of ν_e for maximum growth.

3. Nonlinear Evolution

[9] Simulations of the model have been performed using the parameters of the previous section. The simulations are initialized with a small 1% perturbation in the dust density $n_d(x, y, t = 0) = n_{d0}(1 + 0.01\cos(k_x x))$. The ion density perturbation is chosen to be consistent with dust acoustic waves where $\tilde{n}_i \approx \tilde{n}_d/(1 + k^2\lambda_{Di}^2)$ and $\tilde{n}_d$ and $\tilde{n}_i$ denote the first order density perturbations for the dust and ions. The initial electron density perturbation is taken to be $\tilde{n}_e = 0$. Mode $m = 4$ is initially excited. The mode number is related to the wavenumber by $k_x = 2\pi m/l_x$ where $l_x = 128\lambda_{Di}$ is the system length in the x direction. Also, $l_y = 128\lambda_{Di}$. The growth rate for mode 4 in this case is approximately $\gamma \approx 0.023\omega_{pd}$ from Figure 1a. The dust density is taken to be 100 simulation particles per cell. The applied electric field

$\vec{E}_0$ is in the y direction which produces v_E in the x direction for the background magnetic field in the z direction. The simulation runs for 2×10^4 time steps which corresponds to approximately 4 growth periods of the LFHI or an end time of $\omega_{pd}t = 800$.

[10] Figure 2 shows a summary plot of the electrostatic field energy and dust thermal energy during a simulation. Note that both the x and y electrostatic and thermal energies are shown. In the E_x field energy shown in Figure 2a, it can be seen that the LFHI begins to grow significantly after time $\omega_{pd}t = 100$. During the exponential growth period, good agreement is found between the prediction of Figure 1 and the observed simulation growth rate. Near time $\omega_{pd}t = 300$, the maximum field energy is achieved and the LFHI saturates. This is followed by a period of general decrease in the field energy. It should be reiterated that the E_x field energy, which grows in the direction of the $\vec{E}_0 \times \vec{B}$ drift, indicates the growth of the LFHI dust acoustic type waves. It is important to note that Figure 2a also shows growth in the E_y field energy as well. The y field energy begins to grow near the time of saturation of the x field energy. Therefore, it is seen that an important characteristic of the nonlinear evolution of the LFHI is the production of secondary waves that propagate in a direction perpendicular to the direction of the primary $\vec{E}_0 \times \vec{B}$ drift. This direction is the direction of the $\vec{E} \times \vec{B}$ drift produced by the E_x field of the primary dust acoustic waves.

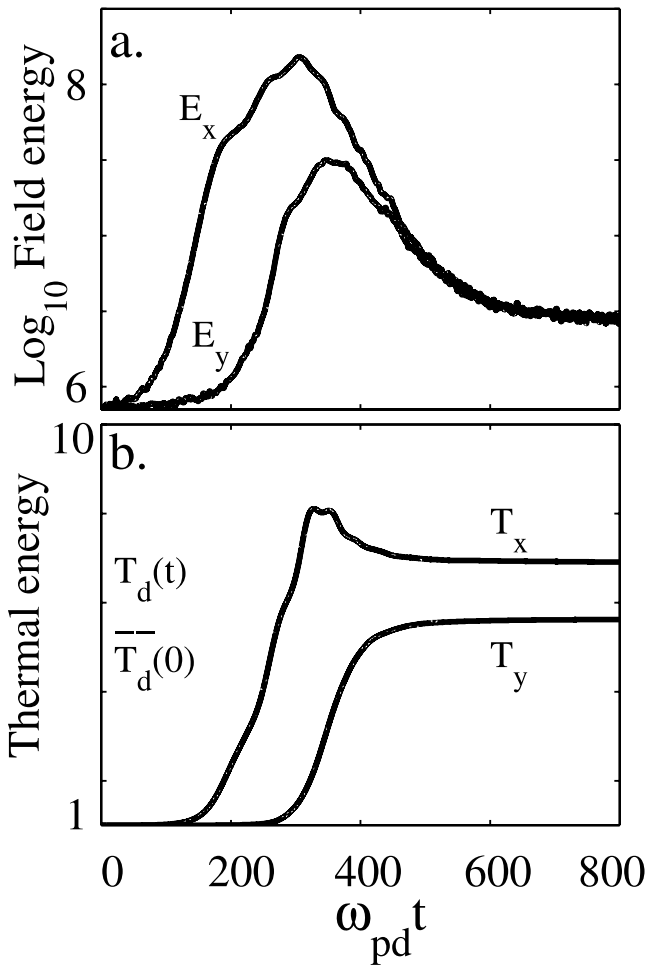

Figure 2. Electric field and dust thermal energy histories during a simulation of the LFHI. Note production of secondary waves (E_y field energy) near saturation ($\omega_{pd}t \approx 300$) and dust heating.

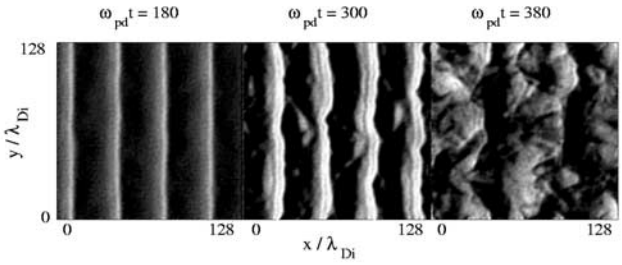

Figure 3. Three dust charge density snapshots during a simulation of the LFHI. Note initial growth of dust acoustic waves propagating in the $+x$ direction then subsequent structuring by secondary wave production.

[11] Figure 2b shows the thermal energy of the dust which indicates that the dust is significantly wave-particle heated by the LFHI. It is noted that there is a gain in thermal energy in both the x and y directions, however, the gain in the x direction is larger and the heating begins in the x direction earlier. The thermal energies saturate roughly after $\omega_{pd}t = 400$ which is after the field energy saturates. The heating of the dust can be seen more clearly in plots of the dust phase spaces which are not shown here. The dust becomes trapped in the wave potentials which ultimately results in significant heating of the dust by the end of the simulation. Also, the dust acquires a small x-directed drift ($v_d \ll v_E$). Nonlinear simulations of the dust acoustic instability [*Winske and Rosenberg*, 1998] show similar behavior.

[12] Figure 3 shows the two-dimensional evolution of the simulation dust density. At the early time $\omega_{pd}t = 180$, the growth of the dust acoustic waves is observed as they propagate in the $+x$ direction. The enhanced regions are just the crests of mode 4 which is initially excited as described earlier. At the intermediate time $\omega_{pd}t = 300$, bending and ripples can be observed in the crests of the primary dust acoustic waves. These are the secondary waves which propagate in the y direction. At late times $\omega_{pd}t = 380$, the plasma is quite turbulent and most of the initial structure of the primary dust acoustic waves is gone. The electron and ion densities show similar behavior.

4. Conclusions

[13] Conclusions can be drawn about how ionospheric parameters control the saturation level of the LFHI. Increasing v_E, or decreasing T_i or T_e results in a higher saturation level. T_i seems to have little effect on the saturation level of the Farley-Buneman instability [*Oppenheim et al.*, 1996], however, T_i is important for the LFHI saturation level since a decrease in T_i changes c_{ds} relative to v_E. Dust parameters are also important in determining the saturation levels of the LFHI. Increase in T_d is observed to reduce the saturation level due to dust Landau damping. Although increasing dust-neutral collisions reduces the linear growth rate when it is roughly ν_{dn}, increasing ν_{dn} is observed to lead to a higher steady state saturation amplitude. This is because the dust

collisions, while cooling the dust, reduce dust Landau damping. This behavior is consistent with past work [*Winske and Rosenberg*, 1998]. When $\nu_{dn} = 0$ as in the previous section, the waves are dust Landau damped after saturation. The current model does not consider the effects of a dust mass distribution, however, a reduction in the saturation amplitude is expected since an increase in mass reduces the linear growth rate.

[14] An important difference in the saturation of the LFHI in comparison to the Farley-Buneman instability seems to be the importance of wave-particle effects. Generation of secondary waves by a secondary Farley-Buneman instability is believed to be its saturation mechanism [*Oppenheim et al.*, 1996; *Otani and Oppenheim*, 1998]. For the parameters used in the current investigation, the dust heating is important in the saturation of the LFHI. A one-dimensional simulation of the LFHI shows higher saturation amplitudes and more dust heating when the secondary y-directed waves are excluded. The dust heating is still observed in the two-dimensional model which indicates that dust heating is important in saturating the LFHI. The secondary waves are likely to be dust acoustic waves produced by a secondary LFHI however these appear not to dominate the saturation of the instability. Basic predictions may be made about possible radar Doppler signatures of the LFHI. It is expected that Doppler spectra of the x-directed (horizontal) waves would exhibit well-defined peaks near the dust acoustic speed while the y-directed (vertical) waves would exhibit a weaker amplitude spectrum with less distinct features. Further calculations are required to provide a more detailed description and will be the subject of future work.

[15] **Acknowledgments.** This work was supported by the Department of Energy under grant DE-FG02-97ER54442. The authors would like to acknowledge stimulating and useful discussions with Marlene Rosenberg.

References

Chae, G. S., W. A. Scales, G. Ganguli, P. A. Bernhardt, and M. Lampe, Numerical model for low frequency ion waves in magnetized dusty plasmas, *IEEE Trans. Plasma Sci.*, *28*, 1694–1705, 2000.

Cho, J. Y. N., and J. Rottger, An updated review of polar mesospheric summer echoes: Observation, theory, and their relationship to noctilucent clouds and subvisible aerosols, *J. Geophys. Res.*, *102*, 2001–2020, 1997.

Havnes, O., et al., First detection of charged dust particles in the Earth's mesosphere, *J. Geophys. Res.*, *101*, 10,839–10,847, 1996.

Kelley, M. C., *The Earth's Ionosphere: Plasma Physics and Electrodynamics*, Academic, San Diego, Calif., 1989.

Kelley, M. C., C. Alcala, and J. Y. N. Cho, Detection of a meteor contrail and meteoric dust in the Earth's upper mesosphere, *J. Atmos. Sol. Terr. Phys.*, *60*, 359–369, 1998.

Oppenheim, M., N. Otani, and C. Ronchi, Saturation of the Farley-Buneman instability via nonlinear electron $\mathbf{E} \times \mathbf{B}$ drifts, *J. Geophys. Res.*, *101*, 17,273–17,286, 1996.

Otani, N., and M. Oppenheim, A saturation mechanism for the Farley-Buneman instability, *Geophys. Res. Lett.*, *25*, 1833–1836, 1998.

Rosenberg, M., and P. K. Shukla, Low-frequency Hall current instability in a dusty plasma, *J. Geophys. Res.*, *105*, 23,135–23,139, 2000.

Rosenberg, M., and P. K. Shukla, Parallel propagation effects on low-frequency Hall current instability in a dusty plasma, *Planet. Space Sci.*, *50*, 261–267, 2002.

Scales, W. A., G. S. Chae, and G. Ganguli, Numerical simulation investigation of dust charging effects on electrostatic ion waves in dusty plasmas, *Phys. Scr. T*, *89*, 142–146, 2001.

Winske, D., and M. Rosenberg, Nonlinear development of the dust acoustic instability in a collisional dusty plasma, *IEEE Trans. Plasma Sci.*, *26*, 92–99, 1998.

G. S. Chae and W. Scales, Electrical and Computer Engineering, Whittemore Hall, Virginia Tech, Blacksburg, VA 24061-0111, USA. (wscales@vt.edu)